Brief Communication

MOLECULAR METABOLISM

HSP70 induces liver X receptor pathway activation and cholesterol reduction *in vitro* and *in vivo*

Burcin Gungor [1,2,6,7], Lauri Vanharanta [1,2,7], Maarit Hölttä-Vuori [1,2], Juho Pirhonen [1,2], Nikolaj H.T. Petersen [3], Silvia Gramolelli [4], Päivi M. Ojala [4,5], Thomas Kirkegaard [3], Elina Ikonen [1,2,*]

ABSTRACT

Objective: Heat Shock Proteins (HSPs) maintain cellular homeostasis under stress. HSP70 represents a major stress-inducible family member and has been identified as a druggable target in inherited cholesterol-sphingolipid storage diseases. We investigated if HSP70 modulates cholesterol accumulation in more common conditions related to atherogenesis.

Methods: We studied the effects of recombinant HSP70 in cholesterol-laden primary macrophages from human blood donors and pharmacological HSP70 upregulation in high-cholesterol diet fed zebrafish.

Results: Recombinant HSP70 facilitated cholesterol removal from primary human macrophage foam cells. RNA sequencing revealed that HSP70 induced a robust transcriptional re-programming, including upregulation of key targets of liver X receptors (LXR), master regulators of whole-body cholesterol removal. Mechanistically, HSP70 interacted with the macrophage LXRalpha promoter, increased LXRalpha and its target mRNAs, and led to elevated levels of key proteins facilitating cholesterol efflux, including ATP-binding cassette transporters A1 and G1. Pharmacological augmentation of endogenous HSP70 in high-cholesterol diet fed zebrafish activated LXR and its target mRNAs and reduced cholesterol storage at the whole organism level.

Conclusion: These data demonstrate that HSP70 exerts a cholesterol lowering effect in primary human cells and animals and uncover a nuclear action of HSP70 in mediating cross-talk between HSP and LXR transcriptional regulation.

Keywords Cholesterol metabolism; Liver X receptor; Heat shock protein; Human macrophages; Transcriptional regulation

1. INTRODUCTION

Heat shock proteins (HSPs) are chaperones that facilitate protein folding and transport, with essential roles in maintaining cell homeostasis and survival [1]. The HSP70 family is evolutionarily the most conserved subfamily, and the major stress-inducible member of this family is HSP70-1 (HSPA1A, hereafter referred to as HSP70). A fraction of HSP70 is released from stressed cells by an unconventional mechanism, possibly involving exosomes and/or secretory lysosomes [2]. In addition to its chaperone function in proteostasis, HSP70 can act as a signaling molecule affecting cytokine production and functional properties of immunocompetent cells via Toll-like receptors [3].

The therapeutic potential of HSP modulation is currently investigated in several diseases, such as cancers and neurogenerative disorders [4,5], but the role of HSPs in cholesterol metabolic regulation is not well understood. The development of atherosclerotic lesions in the arterial intima involves cholesterol accumulation and chronic inflammation. HSPs have been implicated in the process, mostly owing to their immunoinflammatory effects [6]. Some HSPs, such as HSP90, appear to be pro-atherogenic and HSP90 inhibition exerts anti-atherogenic effects in apolipoprotein E-deficient mice [7,8]. In humans, high circulating HSP70 levels are inversely related to the risk of coronary artery disease [9–11] but whether HSP70 has *bona fide* atheromodulatory function(s) is not well understood.

In relation to lipids, HSP70 was shown to bind to the endo/lysosomal phospholipid bis(monoacylglycero)phosphate (BMP), which functions as a cofactor of lysosomal sphingolipid catabolism [12]. Treatment with recombinant HSP70 (rHSP70) reduced lysosomal storage in several sphingolipid storage diseases, suggesting that it provides a potential candidate for their treatment [13]. Interestingly, reduction of sphingolipid storage was accompanied by reduced cholesterol accumulation in Niemann-Pick type C1 (NPC1) patient cells. The NPC1

[1]Department of Anatomy, Faculty of Medicine, University of Helsinki, Haartmaninkatu 8 00290 Helsinki, Finland [2]Minerva Foundation Institute for Medical Research, Tukholmankatu 8, 00290 Helsinki, Finland [3]Orphazyme A/S, Ole Maaløes Vej 3, DK-2200 Copenhagen N, Denmark [4]Research Programs Unit, Translational Cancer Biology, University of Helsinki, Haartmaninkatu 8, 00290 Helsinki, Finland [5]Foundation for the Finnish Cancer Institute, Helsinki, Finland

[6] Current address: Department of Medical Biochemistry, Faculty of Medicine, Istinye University, Maltepe mah. Edirne Cirpici Yolu No: 9 Cevizlibag, 34010 Zeytinburnu-İstanbul, Turkey.

[7] These authors contributed equally to this work.

*Corresponding author. Faculty of Medicine/Anatomy, Haartmaninkatu 8, 00290 Helsinki, Finland. E-mail: elina.ikonen@helsinki.fi (E. Ikonen).

Received June 20, 2019 • Accepted July 3, 2019 • Available online 6 July 2019

https://doi.org/10.1016/j.molmet.2019.07.005

protein is crucial for exporting cholesterol from the endo/lysosomal system [14] and HSP70 was shown to be important for its folding [15]. These findings raise the question if HSP70 has cholesterol lowering potential in more common pathologies related to cholesterol accumulation.

Here, we studied the effects of rHSP70 on human primary monocyte-derived macrophage foam cells that accumulate cholesterol from modified low-density lipoproteins (LDL). Such lesional macrophages play important functions in all aspects of atherosclerosis [16]. We also investigated the functional effects of HSP70-elevating pharmacological compounds in high-cholesterol diet fed zebrafish *in vivo*.

2. MATERIALS AND METHODS

2.1. Cells

Human buffy coat samples were obtained from the Finnish Red Cross (Finnish Red Cross permit numbers 21/2015, 39/2016, 54/2017), in accordance with the Declaration of Helsinki. Peripheral blood mononuclear cells (PBMCs) were isolated by Ficoll layering [17] with Ficoll—Paque Premium (GE Healthcare), and differentiated to macrophages during 7 days *in vitro* cultivation in serum-free macrophage media (Gibco) in the presence of 10 ng/ml of GM-CSF (Invitrogen). Key resources used in the study are summarized in Table S1.

2.2. Recombinant HSP70

Recombinant wild-type HSP70 and the BMP binding deficient mutant W90F-HSP70 were supplied by Orphazyme A/S. A standard final concentration of 300 nM rHSP70 was employed [12], as a 10-fold higher concentration did not further increase the cholesterol reducing effect and a 1: 10 concentration appeared less potent (Figure S1A—D). Endotoxin levels of rHSP70 were determined as 2 EU/mg (by FujiFilm, Billingham, UK), i.e. below the accepted maximum value of 5 EU/mg.

2.3. Cholesterol loading and efflux

PBMC derived macrophages were loaded with 50 μg/ml of acLDL for 3 days in macrophage serum-free medium (Macrophage-SFM), 100 U/ml penicillin, 100 μg/ml streptomycin as described [18], to generate foam cells mimicking early atherosclerotic cholesterol laden macrophages. During the last 16 h of acLDL loading, cells were incubated in the presence of rHSP70 or vehicle control. Cholesterol efflux was performed in complete medium (RPMI containing 10% FBS) for 12 h in the presence or absence of wt or W90F mutant rHSP70. After efflux, cells were washed and collected in PBS. Cells were lysed in RIPA buffer containing protease inhibitors, 2% NaCl, or RNA lysis buffer for protein, lipid and transcript analyses, respectively. For analyzing radiolabeled cholesterol efflux, acLDL (50 μg/ml) was incubated with [^{3}H]cholesterol (1 μCi/ml) in macrophage-SFM for 3 h at room temperature, and then added to macrophages for 3 days. During the last 16 h of loading, rHSP70 was applied to the samples indicated. [^{3}H]-cholesterol efflux to 10% FBS or 6% HDL-enriched serum (prepared by polyethylene glycol precipitation as in [19]) in RPMI was measured for 3 h, as described [19], with rHSP70 present in the samples indicated.

2.4. Zebrafish husbandry, embryo culture and diets

Zebrafish (Danio rerio) larvae of the Turku strain have been maintained in the laboratory for ~20 years. The animal project permit (ESAVI/422/04.10.07/2017) was obtained from the Animal Experiment Board of the Regional State Administrative Agency of Southern Finland. Wild-type zebrafish larvae used in each experiment came from the same breeding batch of fish and had a mixed parentage. Larvae were kept in standard larval medium (5.00 mM NaCl, 0.44 mM $CaCl_2$, 0.33 mM $MgSO_4$ and 0.17 mM KCl; referred to as E3) and raised at 28.5 °C on a 14:10-h light—dark (LD) cycle until harvesting at the indicated time points between 1 and 15 days post fertilization (dpf). Larvae were raised in E3 on a Petri dish. From 5th dpf onwards, larvae were fed either normal diet (ND) (SDS-100, Special Diet Services) or high cholesterol diet (HCD; SDS-100 supplemented with 4% w/w cholesterol, from Sigma Aldrich). Diets were replaced daily for 10 days. The fish were starved for 24 h prior to harvesting. The larvae were terminated mechanically after immersion in ice-cold water.

2.5. HSP70 inducers and their application

17-DMAG was from Invivogen and BGP-15 was from Sigma. 17-DMAG was added to human macrophage foam cells at 500 nM concentration during the last 16 h of acLDL loading and during the 12 h of efflux to complete medium (RPMI containing 10% FBS, analogously to rHSP70 treatment). The inducers were administered together with HCD to the larvae starting from 5th dpf on, at the indicated concentrations. 17-DMAG was dissolved in DMSO and further diluted in E3 before application to the fish. BGP-15 and BM were dissolved in PBS and kept as stock at −20 °C. 17-DMAG was applied every other day, BGP-15 and BM were applied daily; hsp70 mRNA levels were measured after 2 days of drug treatment on normal diet, and the other mRNAs on HCD-fed fish at 15th dpf.

2.6. Western blotting

Protein lysates were cleared by centrifugation at 12000 rpm for 10 min at 4 °C. Protein concentrations were determined using the Bio-Rad protein assay kit, and equal amounts of total protein were loaded on SDS-polyacrylamide gels. Western blots were performed using monoclonal anti-HSP70 (1:3000), polyclonal anti-ABCA1 (1:500), polyclonal anti-NPC1 (1:1000), polyclonal anti-FABP4 (1:2000) and polyclonal anti-GRAMD1A (1:1000). The blots were developed using the Clarity western enhanced chemiluminiscense substrate (Bio Rad). Protein bands were normalized to stained membrane using Proact membrane stain (Amresco). Quantitation of protein bands was performed using ImageJ program (https://imagej.nih.gov/ij/).

2.7. Lipid analysis

Cells were harvested in 2% NaCl. Larvae were pooled in microcentrifuge tubes (5 larvae/condition) and excess water was removed. Larvae were homogenized in 2% NaCl with a pestle, followed by sonication and vigorous vortexing. Lipids were extracted as described [20]. Lipids corresponding to equal amount of protein per sample were separated by thin layer chromatography (TLC) using hexane:diethyl ether:acetic acid, 80:20:1 as running solvent. The TLC plate was charred (exemplary TLC in Figure S1C) and free cholesterol and cholesteryl ester bands quantitated using ImageJ. For analyzing [^{3}H]-cholesterol efflux, radioactivity in medium and in cells was analyzed by liquid scintillation counting after the 3 h efflux and percent efflux was calculated as (radioactivity in medium/radioactivity in cells + medium) ×100%, taking the average of three technical replicates.

2.8. RNA isolation and qRT-PCR

Total RNAs were isolated using NucleoSpin RNA isolation kit (Macherey—Nagel, Cat. 740955-250). Cells were directly lysed using RNA lysis buffer supplied in the kit. For larvae, 7 per condition were pooled and homogenized in RNA lysis buffer by pestle strokes. 1.0 μg of total RNA was transcribed using SuperScript VILO cDNA synthesis kit (Invitrogen). Quantitative reverse transcription PCR (qRT-PCR) was

performed using Light Cycler 480 SYBER Green I Master Mix (Roche) and a Light Cycler 480 II (Roche). Reaction steps; 95 °C 15′ and 40 cycles of 95 °C 15 s, 60 °C 30 s and 72 °C 10 s, for human samples and 95 °C 15' and 40 cycles of 95 °C 5 s, 60 °C 10 s and 72 °C 13 s, for fish samples. ΔΔ Ct method was used to calculate the results. Relative quantities of human mRNAs were normalized to 18S and fish mRNAs to β-actin. The oligonucleotides used for qRT-PCR are provided in Table S2.

2.9. RNA sequencing

RNA samples of macrophage foam cells from 4 individual blood donors, with cholesterol efflux performed in the presence or absence of rHSP70, were used for sequencing. Samples were sequenced with Illumina NextSeq sequencer (Illumina, USA) in one run using Ribo-Zero rRNA removal and NEBNext Ultra Directional RNA Library prep. The sequencing was performed as single end sequencing for read length 75 bp (SE75 or 1 × 75). RNA sequencing results were analyzed using "Gene Set Enrichment Analysis". 3D principal component analysis (PCA) was performed to observe potential differential expression between control and treated groups. 3D PCA plot demonstrated less scattered control sample distribution and sample cohorts separated clearly in the space defined by the 3 first principal components (Figure S2A). Differential expression statistics revealed normalized raw data counts of each sample and the significance of changes in the presence of rHSP0 treatment by adjusted p-values (p adj values) using DeSEQ2 program. Heatmaps were generated with the R heatmap2 function.

2.10. Chromatin immunoprecipitation (ChIP)

Efflux samples with or without rHSP70 treatment were crosslinked with 1% formaldehyde, incubated in 0.125M glycine and lysed in RIPA buffer supplemented with protease (Pierce) and phosphatase (Pierce) inhibitors. Genomic DNA was fragmented in 400—600 bp fragments by sonication using Misonix 3000, lysates were precleared by centrifugation and incubated rotating overnight at 4 °C with 5 μg of anti-HSP70 or 3 μg anti-HA-tag (HA:11, Biolegend) mouse monoclonal antibodies. Protein G-coated magnetic beads (30 μl, Invitrogen) were added to the samples and incubated rotating for 2—4 h at 4 °C, washed once with RIPA buffer, once with RIPA 0.5 M NaCl and once with RIPA 0.25 M LiCl buffer. Washed beads were treated with 10 μg RNAse A for 1 h at 37 °C and with 20 μg Proteinase K at 65 °C overnight. After DNA purification (Macherey—Nagel PCR-purification Kit), the LXRalpha promoter was amplified by qRT-PCR (using primers provided in Table S2). Data were analyzed according to the fold enrichment method, and for each individual, the signals from the HSP70 samples were normalized to the corresponding ones from HA samples.

2.11. Electrophoretic mobility shift assay (EMSA)

To prepare nuclear extracts for EMSA, cells were pelleted and resuspended in ~10 volumes of cell lysis buffer (10 mM Hepes pH 8, 10 mM NaCl, 5 mM $MgCl_2$, 0.5 mM DTT) with added protease inhibitors [chymostatin, leupeptin, antipain, and pepstatin A (all from Sigma—Aldrich) at a final concentration of 25 μg/μl each] and phosphatase inhibitors [activated Na-ortho-vanadate (Sigma—Aldrich) at 2 mmol/l final concentration and NaF (Sigma—Aldrich) at 25 mmol/l final concentration]. After incubating on ice for 30 min, nuclei were pelleted and 1 volume of nuclei lysis buffer was added (10 mM Hepes pH 8, 300 mM KCl, 5 mM $MgCl_2$, 0.5 mM DTT, 20% glycerol and protease and phosphatase inhibitors). Nuclear extracts were incubated for 30 min on a rotating wheel at 4 °C and then centrifuged to remove insoluble pellet. For EMSA reactions, ~2.5 μg of nuclear lysate or 10 ng of rHSP70 was used to analyze binding to biotinylated DNA duplexes harboring the −147-+78 region of LXRalpha promoter. EMSA binding reactions, electrophoresis and blotting were performed by using Gelshift Chemiluminescent EMSA Kit (Active Motif) according to manufacturer's instructions.

2.12. Knockdown experiments in THP-1 macrophages

THP-1 cells (from ATCC) were cultivated in RPMI-1640 medium containing 10% FBS, 1% penicillin/streptomycin/L-glutamine and 25 mM HEPES. Differentiation and nucleofection were performed as previously described [21]. Before electroporation THP-1 monocytes were predifferentiated in growth medium supplemented with 1% sodium pyruvate, 1% nonessential amino acids, 10 ng/ml PMA, and 50 μM β-mercaptoethanol for 48 h. 2.5 × 10E6 cells were transfected with 1 μg of GL2-control siRNA, 1 μg of HSP70 siRNA (SigmaAldrich, Cat. NM005345) or 1 μg of LXRa siRNA (Thermo Fisher, Cat. AM51331) using a nucleofector kit from Lonza (Cat. VPA-1007). After transfection, differentiation was continued for 24 h with 2.5 ng/ml PMA. Differentiated cells were loaded with 50 μg/ml acLDL for 2 days. Non-transfected cells were differentiated continuously for 3 days before acLDL loading. After loading, cholesterol efflux was performed in medium containing 10% FBS. Treatment with 300 nM rHSP70 or 5 μM T0901317 for 16 h before efflux and during 12 h efflux. All samples were collected at the same point for analysis.

2.13. Fluorescence labeling of cells

Alexa 568-labeled rHSP70 was administered to the cells similarly as unlabeled rHSP70. Late endosomal/lysosomal compartments were labeled with Alexa 647 dextran (1:200) (dextran size 1000) (Thermo Fischer) overnight. Lipid droplets were labeled with HCS Lipid TOX Green Neutral Lipid Stain (1:1300) (Thermo Fischer) for 30 min prior to imaging. BODIPY-cholesterol/methyl-β-cyclodextrin complex was prepared as in [22]. Primary macrophage foam cells maintained in 4-well Ibidi slides were labeled with 1:1000 BODIPY-cholesterol/methyl-β-cyclodextrin complex for 5 min at 37 °C after 3 days of acLDL loading. The cells were washed twice with PBS and incubated in serum-free RPMI for 6 h to equilibrate the label. Sterol efflux was performed in 6% HDL-enriched serum prepared as in [23] for 16 h. rHSP70 was present during the last 16 h of acLDL loading, the 6h equilibration and the efflux.

2.14. Imaging and image analysis

For monitoring rHSP70 localization, cells were visualized with a Leica TCS CARS SP8 confocal microscope (Leica, Germany) using a 63× HC PL APO CS2 glycerol objective. Sequential scans were taken to avoid cross-talk between channels. To visualize BODIPY-cholesterol labeling, a fully motorized Nikon Eclipse Ti-E inverted fluorescent microscope with perfect focus system was used (Nikon, Japan). Cells were imaged in a live cell chamber at 37 °C, 5% CO_2. Images were taken every 20 min using a 20× air objective and Andor iXon 897 illuminated EMCCD camera and analyzed by ImageJ configured with a macro plug-in for image segmentation. The average cellular BODIPY intensity was calculated based on image segmentation, efflux rate is an inverse slope of diminishing intensity plotted against time. Zebrafish larvae were stained with LD540 [24] to visualize neutral lipids. On day 15, larvae were collected and fixed in 4% PFA overnight at 4 °C. LD540 (1:10000) was applied to fish overnight at 4 °C. Samples were washed, mounted in 85% glycerol and visualized using Leica TCS CARS SP8 confocal microscope using a 25× water objective.

2.15. Statistical analysis

Graphs were generated using Microsoft Excel or GraphPad Prism 6.0. Data are expressed as mean ± SEM. P values were calculated using two-tailed Student's t-test and statistical significance of the results exhibited as ***: $p < 0.001$; **: $p < 0.01$; *: $p < 0.05$.

3. RESULTS AND DISCUSSION

3.1. Recombinant HSP70 stimulates cholesterol removal from primary human macrophage foam cells

Peripheral blood monocytes from human blood donors were differentiated into macrophages during 7 days and incubated with modified low-density lipoproteins (acetylated LDL, acLDL) for 3 days (Figure 1A). This mimics atherosclerotic foam cell formation and results in a marked increase in the cellular cholesterol content. Free (i.e. unesterified) cholesterol and especially cholesteryl esters, the storage form of cholesterol in lipid droplets, were markedly increased (Figure 1B). Cholesterol removal was induced by referring the cells to 10% serum containing medium. After 12 h of efflux, both free and esterified cholesterol levels were significantly reduced (Figure 1A,B).

To analyze if recombinant HSP70 (rHSP70) can modulate cholesterol removal, the cells were treated with 300 nM rHSP70 for the last 16 h of acLDL loading and during efflux (Figure 1A). This resulted in a ~2-3-fold increase in cellular HSP70 content (Figure 1C). rHSP70 can be taken up via scavenger receptors and enter the lysosomes of recipient cells [12,13,25,26]. In agreement, Alexa Fluor 568-rHSP70 prominently labeled macrophage lysosomes (Figure 1D). Remarkably, rHSP70 enhanced cholesterol removal from macrophage foam cells, as evidenced by the decreased cholesteryl ester content compared to cells incubated in its absence (Figure 1B). A 10-fold higher rHSP70 concentration showed a similar cholesterol reducing efficiency (Figure S1D); therefore, we employed 300 nM rHSP70 in further experiments.

To directly measure cholesterol efflux, cells were incubated with [^{3}H]-cholesterol-labeled acLDL and the partitioning of the radiolabel between cells and efflux medium was analyzed. This showed that rHSP70 stimulated [^{3}H]-cholesterol efflux to both complete serum and HDL-enriched serum acceptors (Figure 1E). To assess cholesterol efflux rate, foam cells were labeled with BODIPY-cholesterol, a fluorescent sterol analog [27,28], and the removal of the fluorescent sterol from cells was followed over time by imaging. This showed that rHSP70 treatment was accompanied by a faster rate of sterol efflux (Figure 1F).

3.2. rHSP70 administration to foam cells results in broad transcriptional re-programming

Considering the lysosomal targeting of rHSP70 in macrophages, we investigated if the effect of rHSP70 on cholesterol efflux in foam cells was mediated via its BMP binding. We found that a mutant rHSP70 (W90F-rHSP70) incapable of interacting with BMP [12,29] induced a similar enhancement of cholesterol efflux as the wt rHSP70 (Figure S1C, D), arguing that BMP binding is not required for this effect.

To further dissect the underlying mechanism, we performed an unbiased transcriptome analysis of acLDL loaded macrophages undergoing cholesterol efflux in the presence or absence of rHSP70 as in Figure 1A. RNA sequencing of macrophage foam cells from four individual blood donors revealed that the rHSP70 induced a major transcriptional reprogramming. These changes were strikingly similar between individuals, with 3D principal component analysis demonstrating a clear separation between treatment groups (Figure S2A). Of the 60 000 transcripts analyzed, ~10% were affected by rHSP70 treatment. Kyoto Encyclopedia of Genes and Genomes (KEGG) pathway enrichment analysis showed multiple pathways to be affected by rHSP70 administration, with 16% of the altered transcripts associated with metabolism (Figure 2A). Importantly, heat map analysis revealed a prominent upregulation of several Liver X Receptor (LXR) target genes (Figures 2B and S2B). In addition, inflammatory and oxidative stress related transcripts were elevated (Figure S2B, C).

3.3. rHSP70 treatment modulates the expression of LXR and LXR targets involved in cholesterol metabolism and trafficking

Quantitative RT-PCR (qRT-PCR) analysis of select targets agreed with the transcript changes observed by RNA sequencing. In particular, the expression of key gatekeepers of cholesterol removal from macrophage foam cells, *ABCA1* and *ABCG1* [30,31], were markedly increased upon rHSP70 treatment (Figure 2B,C). Of note, rHSP70 failed to increase the *ABCA1* mRNA in macrophages not loaded with acLDL (Figure S3A), implying that the effect depends on prior cholesterol challenging of cells. W90F-rHSP70 efficiently upregulated *ABCA1* in loaded cells (Figure S3B), indicating that HSP70 BMP binding is not required.

The increased *ABCA1* mRNA correlated with an increased ABCA1 protein content (Figure 2D), and the combined effect of rHSP70 and acLDL loading on ABCA1 transcript and protein levels was more substantial than that induced by acLDL loading alone (Figure 2C,D). The ABCA1 elevating effect of rHSP70 was highly consistent: altogether, 46 of the 49 blood donors studied (94%) responded to rHSP70 treatment by upregulation of their foam cell *ABCA1* mRNA, and an elevated *ABCA1* content was invariably accompanied by enhanced cholesterol removal from cells. These observations underscore a robust cholesterol reducing potential of rHSP70 on a heterogeneous human genetic background.

The mRNA for the cholesterol-binding protein GRAMD1A was also highly elevated in the presence of rHSP70 (Figure 2B,C) and this was paralleled by strikingly increased GRAMD1A protein levels (Figure 2D). The GRAMD/LAM/Aster proteins regulate nonvesicular cholesterol transport from the plasma membrane to the ER in mammalian cells [32]. Furthermore, a trend for increased NPC1 protein content in rHSP70 treated cells was observed (Figure 2D). This, together with the ABCA1, ABCG1, and GRAMD1A increase speaks for increased cellular cholesterol mobilizing capacity upon rHSP70 treatment. On the other hand, some transcripts, such as that encoding fatty acid binding protein 4 (FABP4), were downregulated by rHSP70 treatment (Figure 2B—D). This agrees with the idea that rHSP70 induces an anti-atherogenic transcriptional program, as FABP4 deficiency has been linked to reduced macrophage accumulation in atherosclerotic plaques and diminished lesion size [33].

3.4. rHSP70 binds to the LXRalpha promoter and induces its expression

Notably, rHSP70 treatment also increased the LXRalpha transcript encoded by the *NR1H3* gene (Figure 2B,C), suggesting that the increase in key LXR target mRNAs is generated by their enhanced synthesis via this transcription factor. Indeed, treatment of foam cells with the transcription inhibitor actinomycin D for the last 4 h of cholesterol efflux abrogated the rHSP70 induced increase in *ABCA1* mRNA (Figure 2E). This implies that HSP70 does not act via mRNA stabilization as in some other settings [34,35] but by activating *LXRalpha* and thereby increasing transcription of its target genes. Accordingly, *LXRalpha* silencing inhibited the rHSP70 induced *ABCA1* upregulation in macrophages (Figure S4). Importantly, LXRalpha appears as a limiting factor for cholesterol efflux in primary human macrophages [36].

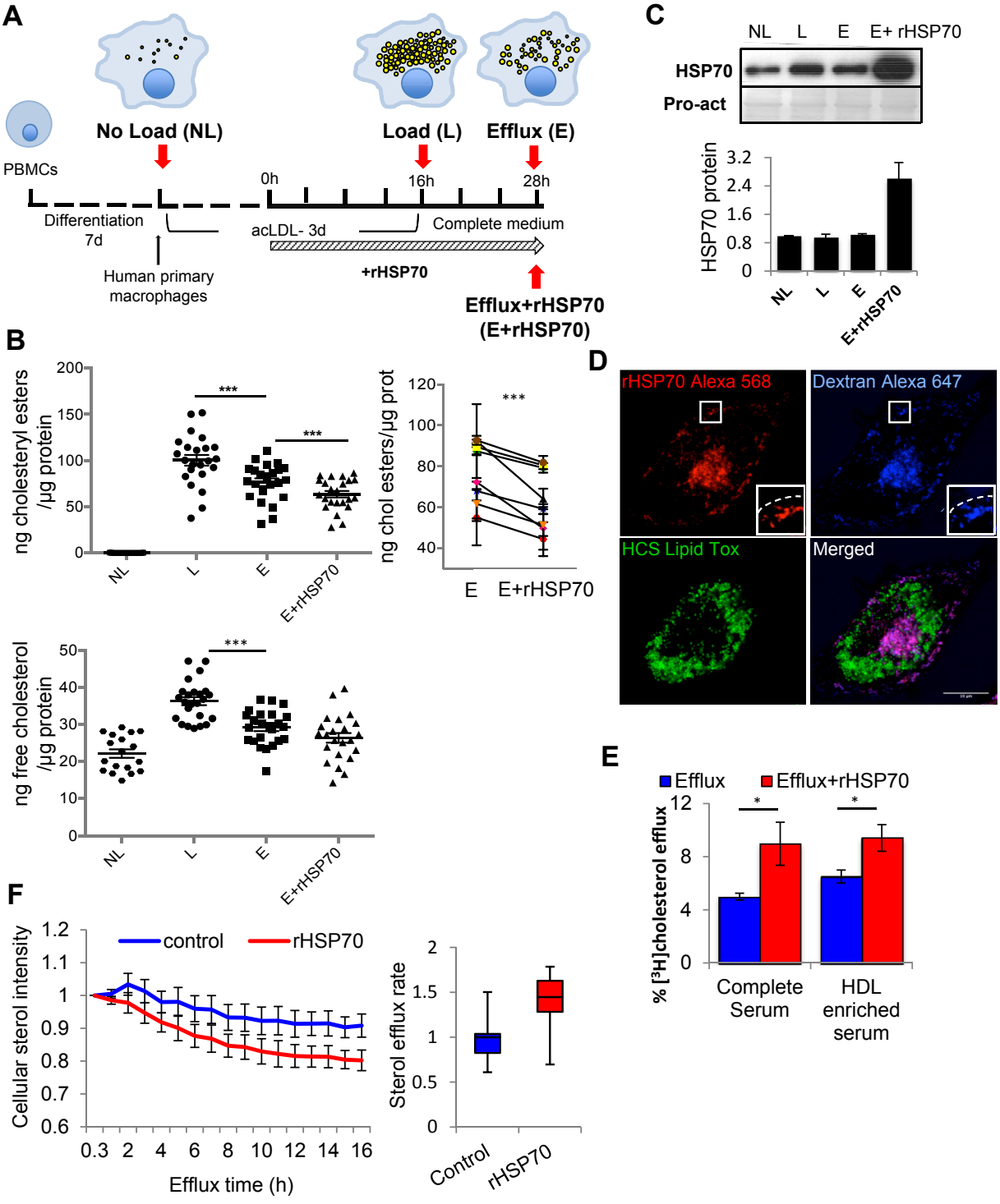

Figure 1: rHSP70 stimulates cholesterol removal from primary human macrophage foam cells. (**A**) Differentiated human macrophages were loaded with 50 µg/ml acLDL for 3 days and cholesterol efflux performed in medium containing 10% FBS −/+ 300 nM rHSP70 for 12 h. Red arrows indicate time points of sample collection. (**B**) Free and esterified cholesterol was analyzed at indicated times and normalized to protein amount. n = 8 donors from 8 experiments with three technical replicates. Change in cholesteryl esters in efflux −/+ rHSP70 is shown for each individual. (**C**) Cells were harvested and proteins separated by SDS-PAGE and analyzed by western blotting using anti-HSP70 antibodies, Pro-act staining as loading control. Band intensities were normalized to NL, n = 6 donors. (**D**) Fluorescence microscopy of foam cells incubated with Alexa 568-labeled rHSP70. Lipid droplets were labeled with Lipid Tox and late endosomal compartments with Alexa-647 dextran. Inset shows late endosomes in the cell periphery, dashed line indicates cell border. Scale bar, 10 µm. (**E**) [^{3}H]cholesterol efflux to complete or HDL-enriched serum from foam cells incubated in the presence or absence of rHSP70 as in 1A. Data from cells of 3 donors with 3 technical replicates. (**F**) BODIPY-cholesterol labeled foam cells were imaged for 16 h −/+ rHSP70. Sterol efflux rate as intensity/cell area/h. Data normalized to control, mean ± SEM. t-test ***: $p < 0.001$; *: $p < 0.05$.

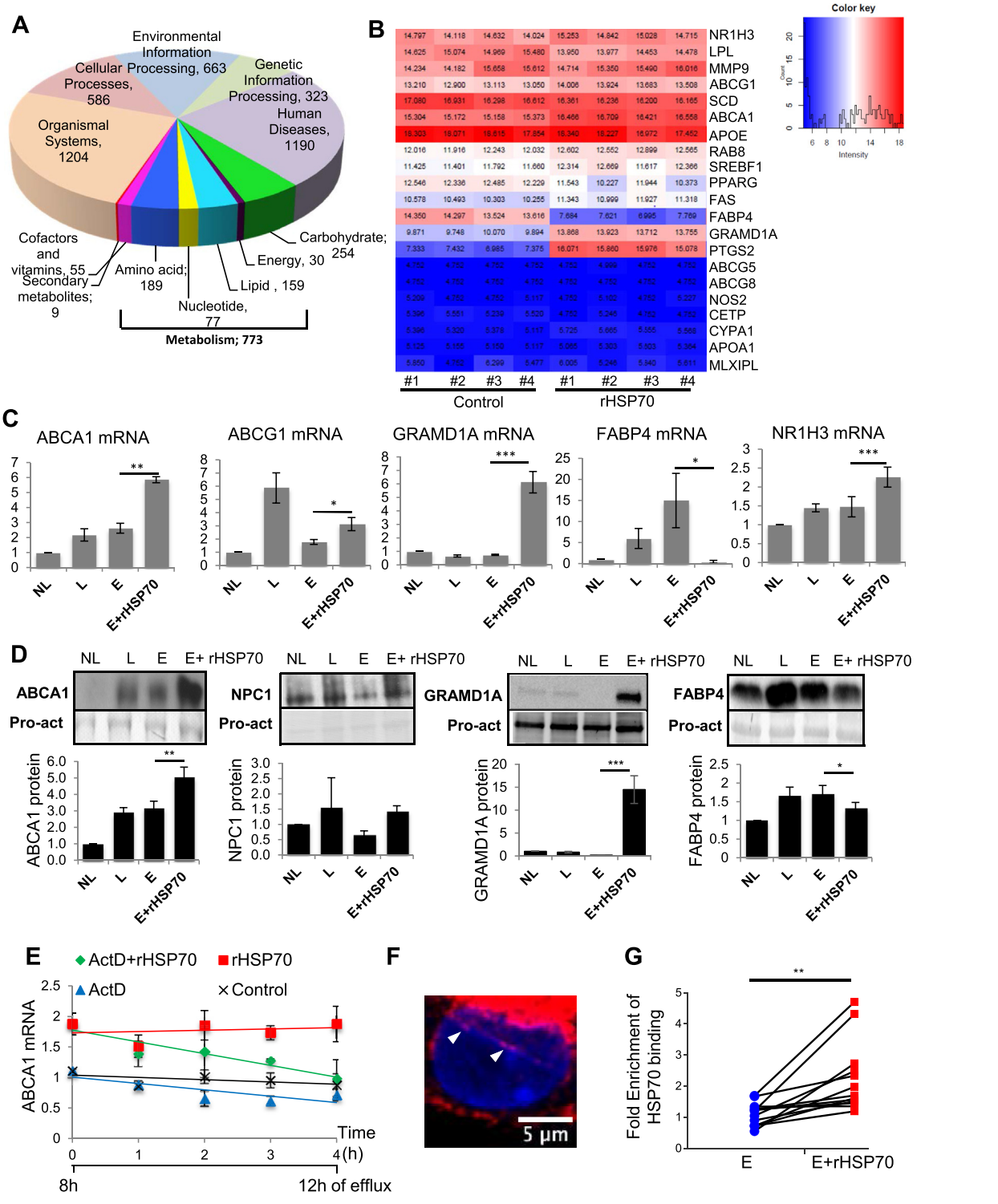

Figure 2: rHSP70 induces broad transcriptional re-programming, interacts with LXRalpha promoter and affects the expression of key macrophage proteins involved in lipid transport. (**A**) Foam cells from 4 blood donors were incubated −/+ rHSP70 during cholesterol efflux and subjected to RNA sequencing. Chart shows relative distribution of genes modulated by rHSP70 using the main KEGG classification of genes, number of affected genes in each class is indicated. (**B**) Heatmap illustrates modulation of lipid metabolism related targets by rHSP70, log2 values of RNA levels in the 4 individuals −/+ rHSP70. See Figure S2B for Ensemble IDs of transcripts. (**C**) Validation of select lipid metabolism related transcripts using qRT-PCR, n = 6 donors with triplicate measurements. (**D**) Western blotting using the indicated antibodies, Pro-act staining as loading control, band intensities normalized to NL. n = 3–7 donors. (**E**) *ABCA1* transcript levels during cholesterol efflux −/+ rHSP70 as in Figure 1A, with last 4 h of efflux −/+ actinomycin D (5 µg/ml), n = 3 donors. Data normalized to control at first time point, mean ± SEM. (**F**) Confocal section of a primary human foam cell incubated with Alexa 568-labeled rHSP70 for 3 h and stained with DAPI, nuclear labeling indicated by arrowheads. (**G**) Chromatin immunoprecipitation in primary human macrophage foam cells using anti-HSP70 antibody or irrelevant anti-HA antibody and amplified by qRT-PCR for LXRalpha proximal promoter region. Fold enrichment over anti-HA control is shown for each of the 13 donors analyzed. Data are mean ± SEM. t-test ***: $p < 0.001$; **: $p < 0.01$; *: $p < 0.05$.

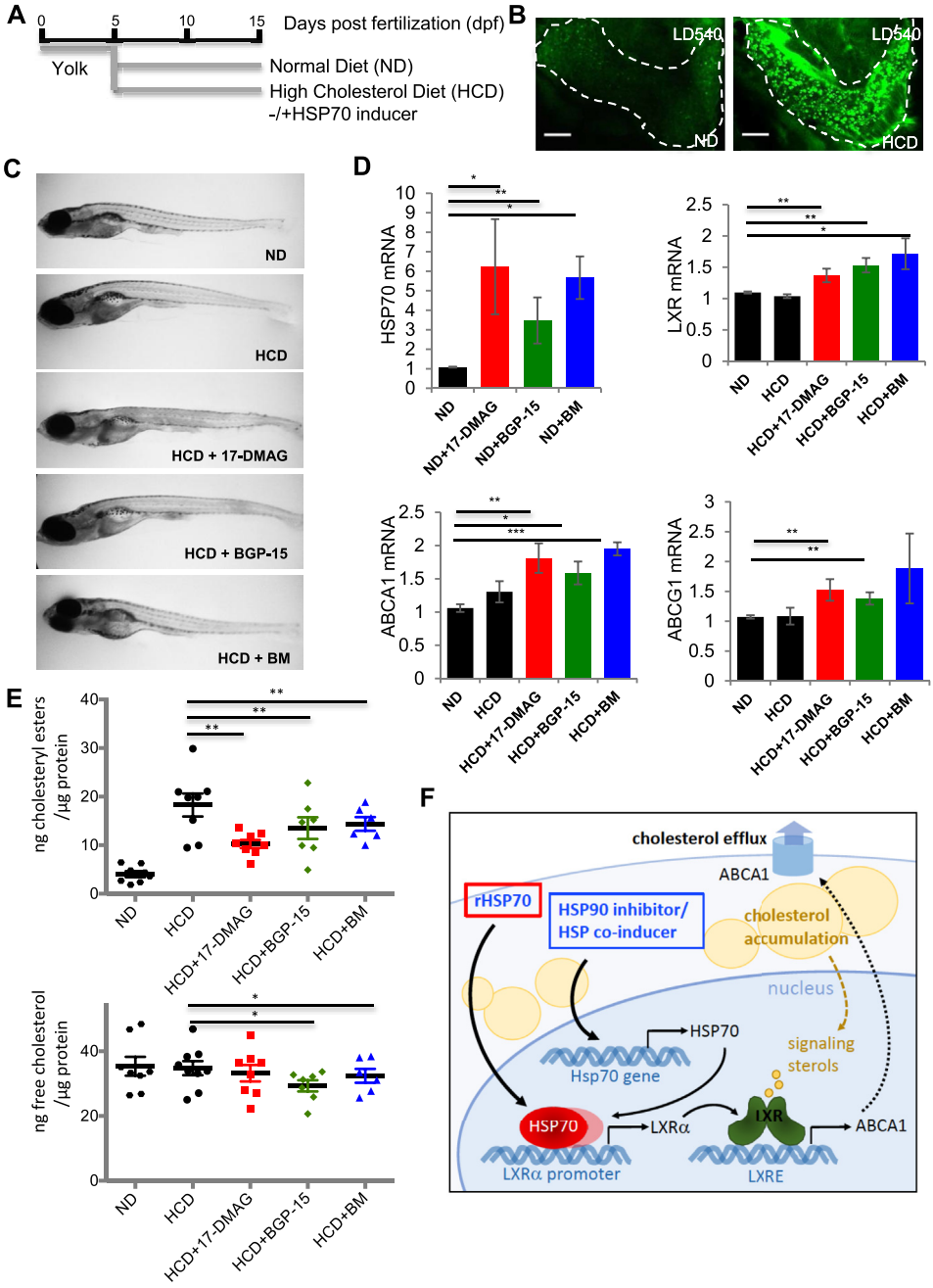

Figure 3: Pharmacological induction of endogenous HSP70 activates LXR and lowers cholesterol in high cholesterol diet fed zebrafish. (**A**) Zebrafish larvae fed with Normal Diet (ND) or High Cholesterol Diet (HCD) for 10 days starting from 5 dpf −/+ HSP70 inducers (1 µM 17-DMAG, 50 µM BGP-15 or 50 µM BM). On day 15, fish were harvested for qRT-PCR or cholesterol determination. (**B**) Lipid accumulation in liver (dashed line) of HCD fed animals visualized by the neutral lipid dye LD540. Scale bar, 50 µm. (**C**) Representative images of fish on day 15. (**D**) *hsp70*, *lxr*, *abca1*, and *abcg1* mRNA levels were measured by qRT-PCR, n = 14 fish/condition, two experiments for hsp70 and n = 20 fish/condition, three experiments for *lxr*, *abca1* and *abcg1*. (**E**) Analysis of fish cholesterol content, each symbol corresponds to a pool of 5 fish, total n = 30–45 fish/condition from three experiments. (**F**) Schematic model. In cholesterol loaded cells, LXR pathway is activated by endogenous sterol ligands, leading to upregulation of LXR targets, such as ABCA1, and stimulation of cholesterol efflux. This process can be boosted by administration of rHSP70 or pharmacological induction of endogenous HSP70, by HSP70 binding to positive regulatory elements in LXRalpha promoter presumably in complex with other proteins and enhancing LXRalpha transcription. Data are mean ± SEM, t-test ***: $p < 0.001$; **: $p < 0.01$; *: $p < 0.05$.

When studying the kinetics of *ABCA1* and *NR1H3* mRNA upregulation, we found that the transcriptional response occurs rapidly, within 3 h upon rHSP70 administration to foam cells (Figure S3C, D). Moreover, a minor fraction of Alexa 568-labeled rHSP70 localized to the nucleus (Figure 2F). To investigate if rHSP70 can associate with the LXRalpha promoter in primary human macrophage foam cells, we collected samples incubated for 3 h with rHSP70 and performed chromatin immunoprecipitation (ChIP) with anti-HSP70 (or anti-HA control) antibodies followed by qRT-PCR of the LXRalpha promoter [37]. This revealed specific binding of HSP70 to the proximal region of the LXRalpha promoter known to contain positive regulatory elements (Figure 2G; no specific binding to *NR1H3* distal region was found, Figure S3E). This finding was corroborated by EMSA demonstrating that while rHSP70 did not directly bind to the proximal region of

the LXRalpha promoter, silencing of endogenous HSP70 abolished the mobility shift induced by binding of nuclear proteins to this area (Figure S3F). The involvement of endogenous HSP70 was also suggested by experiments showing that HSP70 silencing in macrophages abrogates the rHSP70 induced upregulation of the *NR1H3* mRNA (Figure S4). Together, these findings provide the first indication that HSP70 can interact with the macrophage LXRalpha promoter, potentially in co-operation with other *NR1H3* regulators, thereby enhancing its transcription. These data add to the growing list of HSP70 nuclear functions that extend beyond its classical cytoplasmic chaperone activities [38].

3.5. Upregulation of endogenous HSP70 activates the LXR pathway and enhances cholesterol removal in hypercholesterolemic zebrafish

Zebrafish become hypercholesterolemic upon high cholesterol diet (HCD), representing an *in vivo* model for atherosclerosis and liver steatosis studies [39,40]. To induce cholesterol accumulation in zebrafish larvae, we fed them for 10 days with HCD starting from 5 dpf (Figure 3A). This results in pronounced lipid accumulation in tissues (Figure 3B), increased cholesterol storage as cholesteryl esters at the whole animal level (Figure 3E) and upregulation of *hsp7*0 mRNA (Figure S5) as compared to larvae fed with a standard diet.

As further boosting zebrafish HSP70 levels by administering rHSP70 to the swimming water was unsuccessful, we analyzed if pharmacological increase of endogenous HSP70 levels can enhance cholesterol removal. HSP90 inhibitors, such as 17-dimethylaminoethylamino-17-demethoxy-geldanamycin (17-DMAG) disrupt HSP90-HSF complexes, allowing HSF activation and nuclear translocation to transactivate HSP genes [41]. Indeed, we found that 17-DMAG not only increased endogenous HSP70 in primary human foam cells but also ABCA1 protein levels (Figure S6). On the other hand, hydroxylamine derivatives such as O-(2-hydroxy-3-piperidinepropyl)-pyridine-carbonic acid-amidoxime dihydrochloride (BGP-15) and N-[2-hydroxy-3(1-piperidinyl) propoxy]-3 pyridine carboximidoyl-chloride maleate (Bimoclomol, BM) act as HSP co-inducers by amplifying the expression of HSPs induced by mild stress [42].

We administered 17-DMAG, BGP-15 or BM into the zebrafish swimming water, starting concurrently with the onset of HCD feeding (Figure 3A). The compounds did not exhibit toxic effects in the fish (Figure 3C) and were capable of increasing their endogenous *hsp7*0 mRNA levels (Figure 3D). Biochemical analysis of whole fish treated with HCD for 10 days revealed a markedly lower cholesterol content, in particular as cholesteryl esters, in the drug-treated animals (Figure 3E). This was observed with all three compounds, implying that induction of endogenous Hsp70 by several mechanisms exerted a cholesterol-lowering effect *in vivo*. This is likely mechanistically coupled to LXR activation analogously to human foam cell macrophages, as evidenced by the elevated *lxr*, *abca1* and *abcg1* transcript levels in the HCD-fed fish upon HSP70 induction (Figure 3D). Indeed, our findings suggest that the earlier reported atheroprotective effects of 17-DMAG in mice [7,8] may also involve LXR activation.

4. CONCLUSION

Together, this study provides evidence that HSP70 exerts atheroprotective effects *in vitro* and *in vivo* and that this can be mechanistically explained by HSP70 mediated stimulation of the liver X receptor (LXR), the master regulator of whole-body cholesterol removal. HSP70 was found to bind to the LXRalpha promoter, enhance its transcription and boost the expression of key LXR targets under cholesterol loaded conditions (Figure 3F). These findings reveal a function for HSP70 in regulating cholesterol metabolism, uncover a cross-talk between HSP and LXR transcriptional regulation, and suggest that HSP70 induction may provide a treatment paradigm in pathological conditions related to cholesterol accumulation.

AUTHOR CONTRIBUTIONS

EI, BG, PMO, and TK conceived and designed the project, BG, LV, MHV, JP, and SG performed and analyzed the experiments, NHTP, TK, and PMO provided reagents, BG, MHV, TK, LV, and EI wrote the manuscript. All authors commented on and approved the manuscript.

ACKNOWLEDGEMENTS

We thank Anna Uro and Pipsa Kaipainen for technical assistance and HiLIFE infrastructures (Biomedicum Imaging Unit, Zebrafish Unit, Functional Genomics Unit). This study was financially supported by the University of Helsinki, Academy of Finland (grants 282192, 284667, 307415 to E.I.; 307366 to P.M.O. and 309544 to S.G.), Orphazyme A/S, and Sigrid Juselius Foundation (grant to E.I.).

APPENDIX A. SUPPLEMENTARY DATA

Supplementary data to this article can be found online at https://doi.org/10.1016/j.molmet.2019.07.005.

CONFLICT OF INTEREST

TK and NHTP are employees of, and hold shares in Orphazyme A/S.

REFERENCES

[1] Carra, S., Alberti, S., Arrigo, P.A., Benesch, J.L., Benjamin, I.J., Boelens, W., et al., 2017. The growing world of small heat shock proteins: from structure to functions. Cell Stress & Chaperones, 601–611. https://doi.org/10.1007/s12192-017-0787-8.

[2] Radons, J., 2016. The human HSP70 family of chaperones: where do we stand? Cell Stress & Chaperones, 379–404 https://doi.org/10.1007/s12192-016-0676-6.

[3] Asea, A., Kraeft, S.K., Kurt-Jones, E.A., Stevenson, M.A., Chen, L.B., Finberg, R.W., et al., 2000. HSP70 stimulates cytokine production through a CD14-dependant pathway, demonstrating its dual role as a chaperone and cytokine. Nature Medicine 6(4):435–442. https://doi.org/10.1038/74697.

[4] Wu, J., Liu, T., Rios, Z., Mei, Q., Lin, X., Cao, S., 2017. Heat shock proteins and cancer. Trends in Pharmacological Sciences, 226–256. https://doi.org/10.1016/j.tips.2016.11.009.

[5] Kalmar, B., Greensmith, L., 2017. Cellular chaperones as therapeutic targets in ALS to restore protein homeostasis and improve cellular function. Frontiers in Molecular Neuroscience 10:251. https://doi.org/10.3389/fnmol.2017.00251.

[6] Wick, G., Jakic, B., Buszko, M., Wick, M.C., Grundtman, C., 2014. The role of heat shock proteins in atherosclerosis. Nature Reviews Cardiology 11(9):516–529. https://doi.org/10.1038/nrcardio.2014.91.

[7] Madrigal-Matute, J., López-Franco, O., Blanco-Colio, L.M., Muñoz-García, B., Ramos-Mozo, P., Ortega, L., et al., 2010. Heat shock protein 90 inhibitors attenuate inflammatory responses in atherosclerosis. Cardiovascular Research 86(2):330–337. https://doi.org/10.1093/cvr/cvq046.

[8] Lazaro, I., Oguiza, A., Recio, C., Mallavia, B., Madrigal-Matute, J., Blanco, J., et al., 2015. Targeting HSP90 ameliorates nephropathy and atherosclerosis through suppression of NF-κB and STAT signaling pathways in diabetic mice. Diabetes 64(10):3600–3613. https://doi.org/10.2337/db14-1926.

[9] Pockley, A.G., Calderwood, S.K., Multhoff, G., 2009. The atheroprotective properties of Hsp70: a role for Hsp70-endothelial interactions? Cell Stress & Chaperones, 545–553 https://doi.org/10.1007/s12192-009-0113-1.

[10] Dulin, E., García-Barreno, P., Guisasola, M.C., 2010. Extracellular heat shock protein 70 (HSPA1A) and classical vascular risk factors in a general population. Cell Stress & Chaperones 15(6):929–937. https://doi.org/10.1007/s12192-010-0201-2.

[11] Zhu, J., Quyyumi, A.A., Wu, H., Csako, G., Rott, D., Zalles-Ganley, A., et al., 2003. Increased serum levels of heat shock protein 70 are associated with low risk of coronary artery disease. Arteriosclerosis, Thrombosis, and Vascular Biology 23(6):1055–1059. https://doi.org/10.1161/01.ATV.0000074899.60898.FD.

[12] Kirkegaard, T., Roth, A.G., Petersen, N.H.T., Mahalka, A.K., Olsen, O.D., Moilanen, I., et al., 2010. Hsp70 stabilizes lysosomes and reverts Niemann-Pick disease-associated lysosomal pathology. Nature 463(7280):549–553. https://doi.org/10.1038/nature08710.

[13] Kirkegaard, T., Gray, J., Priestman, D.A., Wallom, K.L., Atkins, J., Olsen, O.D., et al., 2016. Heat shock protein-based therapy as a potential candidate for treating the sphingolipidoses. Science Translational Medicine 8(355). https://doi.org/10.1126/scitranslmed.aad9823, 355ra118-355ra118.

[14] Ikonen, E., 2018. Mechanisms of cellular cholesterol compartmentalization: recent insights. Current Opinion in Cell Biology, 77–83. https://doi.org/10.1016/j.ceb.2018.06.002.

[15] Nakasone, N., Nakamura, Y.S., Higaki, K., Oumi, N., Ohno, K., Ninomiya, H., 2014. Endoplasmic reticulum-associated degradation of Niemann-Pick C1: evidence for the role of heat shock proteins and identification of lysine residues that accept ubiquitin. Journal of Biological Chemistry 289(28):19714–19725. https://doi.org/10.1074/jbc.M114.549915.

[16] Tabas, I., Bornfeldt, K.E., 2016. Macrophage phenotype and function in different stages of atherosclerosis. Circulation Research 118(4):653–667. https://doi.org/10.1161/CIRCRESAHA.115.306256.

[17] BOYUM, A., 1964. Separation of white blood cells. Nature 204:793–794.

[18] Blom, T., Bäck, N., Mutka, A.L., Bittman, R., Li, Z., De Lera, A., et al., 2010. FTY720 stimulates 27-hydroxycholesterol production and confers atheroprotective effects in human primary macrophages. Circulation Research 106(4):720–729. https://doi.org/10.1161/CIRCRESAHA.109.204396.

[19] de la Llera-Moya, M., Drazul-Schrader, D., Asztalos, B.F., Cuchel, M., Rader, D.J., Rothblat, G.H., 2010. The ability to promote efflux via ABCA1 determines the capacity of serum specimens with similar high-density lipoprotein cholesterol to remove cholesterol from macrophages. Arteriosclerosis, Thrombosis, and Vascular Biology 30(4):796–801. https://doi.org/10.1161/ATVBAHA.109.199158.

[20] Bligh, E.G., Dyer, W.J., 1959. A rapid method of total lipid extraction and purification. Canadian Journal of Biochemistry and Physiology 37(8):911–917. https://doi.org/10.1139/o59-099.

[21] Maeß, M.B., Wittig, B., Lorkowski, S., 2014. Highly efficient transfection of human THP-1 macrophages by nucleofection. Journal of Visualized Experiments 91:e51960. https://doi.org/10.3791/51960.

[22] Jansen, M., Ohsaki, Y., Rita Rega, L., Bittman, R., Olkkonen, V.M., Ikonen, E., 2011. Role of ORPs in sterol transport from plasma membrane to ER and lipid droplets in mammalian cells. Traffic 12(2):218–231. https://doi.org/10.1111/j.1600-0854.2010.01142.x.

[23] Asztalos, B.F., de la Llera-Moya, M., Dallal, G.E., Horvath, K.V., Schaefer, E.J., Rothblat, G.H., 2005. Differential effects of HDL subpopulations on cellular ABCA1- and SR-BI-mediated cholesterol efflux. Journal of Lipid Research 46(10):2246–2253. https://doi.org/10.1194/jlr.M500187-JLR200.

[24] Spandl, J., White, D.J., Peychl, J., Thiele, C., 2009. Live cell multicolor imaging of lipid droplets with a new dye, LD540. Traffic 10(11):1579–1584. https://doi.org/10.1111/j.1600-0854.2009.00980.x.

[25] Asea, A., Rehli, M., Kabingu, E., Boch, J.A., Bare, O., Auron, P.E., et al., 2002. Novel signal transduction pathway utilized by extracellular HSP70: role of toll-like receptor (TLR) 2 and TLR4. The Journal of Biological Chemistry 277(17):15028–15034. https://doi.org/10.1074/jbc.M200497200.

[26] Murshid, A., Theriault, J., Gong, J., Calderwood, S.K., 2011. Investigating receptors for extracellular heat shock proteins. Methods in Molecular Biology 787:289–302. https://doi.org/10.1007/978-1-61779-295-3_22.

[27] Sankaranarayanan, S., Kellner-Weibel, G., de la Llera-Moya, M., Phillips, M.C., Asztalos, B.F., Bittman, R., et al., 2011. A sensitive assay for ABCA1-mediated cholesterol efflux using BODIPY-cholesterol. Journal of Lipid Research 52(12):2332–2340. https://doi.org/10.1194/jlr.D018051.

[28] Hölttä-Vuori, M., Uronen, R.L., Repakova, J., Salonen, E., Vattulainen, I., Panula, P., et al., 2008. BODIPY-cholesterol: a new tool to visualize sterol trafficking in living cells and organisms. Traffic 9(11):1839–1849. https://doi.org/10.1111/j.1600-0854.2008.00801.x.

[29] Mahalka, A.K., Kirkegaard, T., Jukola, L.T.I., Jäättelä, M., Kinnunen, P.K.J., 2014. Human heat shock protein 70 (Hsp70) as a peripheral membrane protein. Biochimica et Biophysica Acta - Biomembranes 1838(5):1344–1361. https://doi.org/10.1016/j.bbamem.2014.01.022.

[30] Phillips, M.C., 2014. Molecular mechanisms of cellular cholesterol efflux. Journal of Biological Chemistry, 24020–24029. https://doi.org/10.1074/jbc.R114.583658.

[31] Westerterp, M., Bochem, A.E., Yvan-Charvet, L., Murphy, A.J., Wang, N., Tall, A.R., 2014. ATP-binding cassette transporters, atherosclerosis, and inflammation. Circulation Research, 157–170. https://doi.org/10.1161/CIRCRESAHA.114.300738.

[32] Sandhu, J., Li, S., Fairall, L., Pfisterer, S.G., Gurnett, J.E., Xiao, X., et al., 2018. Aster proteins facilitate nonvesicular plasma membrane to ER cholesterol transport in mammalian cells. Cell 175(2). https://doi.org/10.1016/j.cell.2018.08.033, 514–529.e20.

[33] Hotamisligil, G.S., Bernlohr, D.A., 2015. Metabolic functions of FABPs - mechanisms and therapeutic implications. Nature Reviews Endocrinology, 592–605. https://doi.org/10.1038/nrendo.2015.122.

[34] Laroia, G., Cuesta, R., Brewer, G., Schneider, R.J., 1999. Control of mRNA decay by heat shock-ubiquitin-proteasome pathway. Science (New York, N.Y.) 284(5413):499–502. https://doi.org/10.1126/SCIENCE.284.5413.499.

[35] Walters, R.W., Parker, R., 2015. Coupling of ribostasis and proteostasis: hsp70 proteins in mRNA metabolism. Trends in Biochemical Sciences 40(10):552–559. https://doi.org/10.1016/j.tibs.2015.08.004.

[36] Ishibashi, M., Filomenko, R., Rebe, C., Chevriaux, A., Varin, A., Derangere, V., et al., 2013. Knock-down of the oxysterol receptor LXRa impairs cholesterol efflux in human primary macrophages: lack of compensation by LXRb activation. Biochemical Pharmacology 86(1):122–129. https://doi.org/10.1016/j.bcp.2012.12.024.

[37] Theofilatos, D., Anestis, A., Hashimoto, K., Kardassis, D., 2016. Transcriptional regulation of the human liver X receptor α gene by hepatocyte nuclear factor 4α. Biochemical and Biophysical Research Communications 469(3):573–579 https://doi.org/10.1016/j.bbrc.2015.12.031.

[38] Imamoto, N., 2018. Heat stress-induced nuclear transport mediated by Hikeshi confers nuclear function of Hsp70s. Current Opinion in Cell Biology, 82–87. https://doi.org/10.1016/j.ceb.2018.02.010.

[39] Dai, W., Wang, K., Zheng, X., Chen, X., Zhang, W., Zhang, Y., et al., 2015. High fat plus high cholesterol diet lead to hepatic steatosis in zebrafish larvae: a novel model for screening anti-hepatic steatosis drugs. Nutrition and Metabolism 12(1):42. https://doi.org/10.1186/s12986-015-0036-z.

[40] Stoletov, K., Fang, L., Choi, S.H., Hartvigsen, K., Hansen, L.F., Hall, C., et al., 2009. Vascular lipid accumulation, lipoprotein oxidation, and macrophage lipid uptake in hypercholesterolemic zebrafish. Circulation Research 104(8):952–960. https://doi.org/10.1161/CIRCRESAHA.108.189803.

[41] Taipale, M., Jarosz, D.F., Lindquist, S., 2010. HSP90 at the hub of protein homeostasis: emerging mechanistic insights. Nature Reviews Molecular Cell Biology 11(7):515–528. https://doi.org/10.1038/nrm2918.

[42] Crul, T., Toth, N., Piotto, S., Literati-Nagy, P., Tory, K., Haldimann, P., et al., 2012. Hydroximic acid derivatives: pleiotropic hsp Co-inducers restoring homeostasis and robustness. Current Pharmaceutical Design 19(3):309–346. https://doi.org/10.2174/1381612811306030309.

